

# Studies on pH-dependent color variation and decomposition mechanism of Brilliant Green dye in Fenton reaction

Ch. Venkatanarasimha Rao<sup>1</sup> · Ardendu Sekhar Giri<sup>1</sup> · Vibhav V. Goud<sup>1</sup> · Animes Kumar Golder<sup>1</sup>

Received: 7 April 2015 / Accepted: 7 October 2015 / Published online: 7 November 2015  
© The Author(s) 2015. This article is published with open access at Springerlink.com

**Abstract** Degradation of Brilliant Green (BG) dye has been studied using Fenton reagent in the dark environment. The intensity of dye color was pH dependent with maximum absorbance at pH 6. *N*-de-alkylation caused dye decomposition which resulted in the reduction of absorbance. The rate of BG dye decolorization increased with an increase in the H<sub>2</sub>O<sub>2</sub> and Fe<sup>2+</sup> concentration. The presence of background ions commonly found in an industrial dyeing wastewater suppressed the efficiency of color, COD and TOC removal within 9 %. There was about 2.9-fold increase in biodegradability index after 30 min of reaction. The proposed mechanism showed the routes of dye degradation with low errors (−0.88 to 0.49 g mol<sup>−1</sup>) with respect to the exact mass. Dye degradation began with *N*-de-ethylation, and later was further cleaved to aromatic-amine, -acid, -alcohol and -additive products. Hydroquinone was originated by hydroxylation of *N,N*-diethyl aniline. An equilibrium cycle among quinone, hydroquinone and Fe(III)-hydroquinone was exhibited through the formation of charge transfer complex.

**Keywords** Background ions · Biodegradability index · Reaction pathways · Iron-organic complexes

## Introduction

Dyes are used as coloring agents in many industries like textile, plastic, cosmetic, food and paper [1, 2]. They generate effluents containing various types of dyes and pigments. Such effluents are frequently discharged into natural water bodies with and without proper treatment. Dye effluents are characterized by fluctuating pH with high suspended solids and oxygen demand [3]. It also retains the color even after conventional treatments such as biological, adsorption, coagulation, floatation and membrane filtration [4]. Dyes are usually difficult to biodegrade. A large degree of aromaticity present in modern dye molecules increases stability, and conventional biological treatments are ineffective for decolorization and degradation [5, 6]. Furthermore, a large fraction of dyes is adsorbed on the sludge and is not degraded. Ozonation and chlorination are also used for the removal of certain dyes, but at slower rates [7, 8]. They often have high operating costs and limited effect on carbon content [7]. Advanced oxidation processes (AOPs) are potential to overcome many of these limitations. Among different AOPs, Fenton process is one of the most powerful oxidative treatments operated at room temperature and pressure. Fenton's reagent is a mixture of Fe<sup>2+</sup> and H<sub>2</sub>O<sub>2</sub> generating •OH radicals. Fe<sup>2+</sup> initiate and catalyze H<sub>2</sub>O<sub>2</sub> decomposition resulting in the generation of •OH through a complex reaction sequence in an aqueous solution. •OH radicals formed thus cause unselective oxidation of various types of pollutants such as textile dyes, pharmaceutical wastes and other complex organic pollutants in a short reaction time [8]. Hydroxylated and carboxylic derivatives are transformed into H<sub>2</sub>O and CO<sub>2</sub> [9]. Moreover, •OH is converted to OH<sup>−</sup> forming Fe<sup>3+</sup> in Fenton reaction. The rate constant of this

**Electronic supplementary material** The online version of this article (doi:10.1007/s40090-015-0060-x) contains supplementary material, which is available to authorized users.

✉ Animes Kumar Golder  
animes@iitg.ernet.in

<sup>1</sup> Department of Chemical Engineering, Indian Institute of Technology Guwahati, Guwahati, Assam 781039, India

reaction is a few orders higher in magnitude than the Fenton reaction.  $\text{Fe}^{2+}$  is regenerated in small quantity yielding hydroperoxyl radical ( $\bullet\text{OOH}$ ).  $\bullet\text{OH}$  scavenging by  $\text{H}_2\text{O}_2$  at  $\text{pH} < 3$  could form  $\bullet\text{OOH}$  of low oxidation potential (1.7 V vs. SHE) [10].

Fenton oxidation sometimes gives inefficient degradation because of iron-organic complexes [11, 12]. Liu et al. [13] investigated the effect of four flavonoids, i.e., baicilin, luteolin, naringenin, and quercetin suppressing the rate of Fenton reaction. They used the electrochemically reduced iron(III)-ATP complex at a minimum ratio of flavonoid to iron of 1.5:1 at  $\text{pH} 7.4$ . The rate is suppressed in the order as, quercetin > luteolin > naringenin > baicilin. The catechol group in quercetin and luteolin structure enhances iron chelation. Roy et al. [14] proposed a possible degradation mechanism of tropaeolin using iron under oxidizing conditions. Iron-chelate complexes, as well as hydroquinone and quinone compounds, are also identified by mass spectroscopy.

Approximately, 50–70 % of azo dyes consist of the anthraquinone group. They are found in various categories, i.e., acid, basic, disperse, azoic and pigments [8]. Some azo dyes and their precursors have shown to be or are suspected to be human carcinogens [15]. Brilliant Green (BG) is a cationic dye, extensively used in paper printing and textile dyeing [2]. BG dye causes eye burns, irritation to the gastrointestinal tract and skin irritation with redness and pain [2, 16]. The symptoms also include shortness of breath and cough.

Studies on the removal of BG dye include adsorption using modified kaolin clay [17], combinations of sonolysis, photolysis and microwave processes [18], ozonation using micro-bubbles [19] and Fenton-like process ( $\text{Fe}^{3+}/\text{H}_2\text{O}_2$ ) [20].

The routes of BG cleavage is dependent on the target sites of  $\bullet\text{OH}$  radicals. The central carbon atom of BG dye is the most preferred site of  $\bullet\text{OH}$  attack because of its nucleophilic character. Quinone and hydroquinone derivate could form during BG dye decomposition. Likewise, an experimental study is undertaken to investigate the oxidative degradation of BG dye in Fenton reaction. The influence of  $\text{pH}$  and  $\text{Fe}^{2+}$  to  $\text{H}_2\text{O}_2$  mol ratio on color, mineralization, and biodegradability index also has been studied. The mechanism of dye decomposition is proposed and supported with respect to the exact mass-to-charge ratio appeared in the mass spectra which is not yet reported for Fenton process. A route of iron chelation with hydroquinone molecule is established. Furthermore, BG dye solution was spiked with different background species comparable with the industrial effluent to uncover the impact on the removal kinetics and degradation mechanism.

## Materials and methods

### Reagents

All chemicals and reagents were procured from Merck, India. The purity of BG dye is 90 % (molecular formula:  $\text{C}_{27}\text{H}_{33}\text{N}_2\text{HO}_4\text{S}$ , molecular weight:  $482.64 \text{ g mol}^{-1}$ ). Deionized (DI) water of Millipore, USA (model: Elix-3) was used for reagent and dye solution preparations. Ferrous ammonium sulfate hexahydrate [FAS,  $(\text{NH}_4)_2\text{SO}_4\text{FeSO}_4 \cdot 6\text{H}_2\text{O}$ ] (purity 98.5 %, w/w) and  $\text{H}_2\text{O}_2$  (purity 30 %, v/v) were employed for making of Fenton reagent. The stock solution of 0.1 M  $\text{Fe}^{2+}$  was prepared by dissolving an appropriate amount of FAS in DI water.  $\text{H}_2\text{SO}_4$  solution of 0.1 M was added to lower down the solution  $\text{pH} < 1.5$  to avoid  $\text{Fe}^{2+}$ – $\text{Fe}^{3+}$  conversion and precipitation. The fresh FAS solution was prepared weekly.  $\text{K}_2\text{Cr}_2\text{O}_7$ ,  $\text{AgSO}_4$ , and  $\text{HgSO}_4$  were of 99.9, 98.5 and 99 % purities (w/w). An equal volume of 0.2 M dibasic sodium phosphate ( $\text{Na}_2\text{HPO}_4$ , 97 % purity, w/w) and 0.2 M monobasic sodium phosphate ( $\text{NaH}_2\text{PO}_4$ , 97 % purity, w/w) were mixed to obtain the buffer solution of  $\text{pH} 6$ . It was used to raise the solution  $\text{pH}$  to terminate the Fenton reaction as well as to maintain  $\text{pH}$  before absorbance measurement.

### Analytical techniques

BG concentration was determined using an UV–Vis Spectrophotometer of Thermo Scientific, India (model: UV 2300). The solution was scanned in the range from 200 to 800 nm, and the maximum absorbance was found at 623 nm. Solution  $\text{pH}$  was measured using a precision  $\text{pH}$  meter of Eutech Instruments, Malaysia (model:  $\text{pH}/\text{ion} 510$ ). Determination of chemical oxygen demand (COD) was performed according to HACH method. A closed reflux digester of HACH, USA (model: DRB 200) was used for digestion. Mineralization of BG dye was monitored on the basis of total organic carbon (TOC) measurement (TOC analyzer, model: Aurora 1030C, O.I. Analytical, USA). 5-day biological oxygen demand ( $\text{BOD}_5$ ) was determined using the bottle incubation method. The following mineral basis ( $\text{g L}^{-1}$ ) was used for the  $\text{BOD}_5$  test:  $\text{MgSO}_4 \cdot 7\text{H}_2\text{O}$  22.5,  $\text{CaCl}_2$  27.5,  $\text{FeCl}_3$  0.15,  $\text{NH}_4\text{Cl}$  1.7,  $\text{Na}_2\text{HPO}_4 \cdot 7\text{H}_2\text{O}$  33.4 and  $\text{K}_2\text{HPO}_4$  8.5.

The identification of BG dye fragments was carried out by a liquid chromatography–time-of-flight mass spectrometry (LC–TOF-MS) (Waters Q-ToF Premier and Acquity UPLC). The chromatographic separation was performed on a YMC Hydrosphere  $\text{C}_{18}$  reverse phase column ( $4.6 \text{ mm} \times 150 \text{ mm}$ ,  $5 \mu\text{m}$  particle size) following a guard column ( $4 \text{ mm} \times 10 \text{ mm}$ ,  $5 \mu\text{m}$  particle size). A mobile phase flow rate of  $0.8 \text{ mL min}^{-1}$  was employed at  $25 \text{ }^\circ\text{C}$ . DI

water and acetonitrile were used as the mobile phase consisting of 0.1 % (v/v) formic acid. A linear gradient of 95–50 % H<sub>2</sub>O was applied over 10 min. A 10  $\mu$ L of both sample and calibration solution were injected from an auto-injector. The samples were analyzed by electrospray ionization method in positive ion mode over the mass range of 100–400 amu. The parent ion was fragmented on the basis of a suitable range of mass-to-charge ( $m/z$ ) ratio. Daughter ions were again selected for further fragmentation.

## Experimental procedure

A cylindrical borosilicate glass beaker (1 L) was used as the reactor. Fenton oxidation was carried out with 400 mL dye solution with an initial concentration of 50 mg L<sup>-1</sup> (0.106 mM) in batch mode. An exalted temperature generally increases the rate of contaminant degradation. On the other hand, it also accelerates H<sub>2</sub>O<sub>2</sub> decomposition even at 60 °C [21, 22]. The study was performed at room temperature (25  $\pm$  2 °C) from the application point of view. The mass concentrations (millimolar concentration in parenthesis) of Fe<sup>2+</sup> and H<sub>2</sub>O<sub>2</sub> were varied from 1–56 (0.25–1) to 170–340 mg L<sup>-1</sup> (5–10), respectively. pH was varied from 2 to 6. Solution pH was adjusted using 0.1 N H<sub>2</sub>SO<sub>4</sub>, and Fe<sup>2+</sup> was mixed for about 5 min. Agitation was continued at 270 rpm using a magnetic stirrer (stirrer bar: length 40 mm,  $\varnothing$  0.8 mm) of Tarson, India (model: Spinnot). H<sub>2</sub>O<sub>2</sub> was then added into solution and samples were taken out at selected intervals of time. pH was raised to 6 with phosphate buffer to stop the reaction by  $\bullet$ OH scavenging at elevated pH, and it also made Fe<sup>2+</sup> unavailability by converting into Fe<sup>3+</sup>. Iron flocs were then separated by centrifugation at 1600 rpm for 20 min. Supernatant was analyzed for dye content, pH, COD, TOC, and BOD<sub>5</sub> values. In addition to that, the supernatant was also filtered using 0.45  $\mu$ m cellulose filter (serial no. 08091ID0683, Pall India Pvt Ltd. India), before LC–MS analysis. The supernatant was heated at 80 °C for about 1 h on a hot water bath to eliminate residual H<sub>2</sub>O<sub>2</sub>, if any, to minimize the interference with COD, TOC, and BOD<sub>5</sub> determinations [20]. All the experiments were repeated and error bars with respect to the mean values are included in the figures.

## Results and discussion

### Effect of pH on variation of color intensity

Brilliant Green is a cationic dye, and its intensity of the color depends on solution pH. The effect of solution pH on the light absorbency of BG dye was studied in the pH range from 1 to 8. Dye concentration was maintained at

4 mg L<sup>-1</sup>. The results are illustrated in Fig. 1. It was observed that absorbance increased with the rise of solution pH and reached a maximum at pH 6 (Fig. 1, inset). Further, the increase in solution pH resulted in the reduction of its absorbance. At pH  $\leq$  2, BG dye solution became almost colorless.

The variation of color intensity was due to its extended conjugated system of alternate double and single bonds. At higher pH, the reaction occurs between OH<sup>-</sup> ion and BG molecule with the disruption of conjugation (Fig. 2). The central carbon atom of BG acts as an electrophilic center and the addition of OH<sup>-</sup> is likely favored and, so the intensity of color decreased with the increase in pH. The rate of color disappearance of BG dye was faster in alkaline medium because of its high nucleophilic character. Decolorization can also occur via nucleophilic attack by H<sub>3</sub>O<sup>+</sup> but a slower rate in a mild acidic medium. H<sub>3</sub>O<sup>+</sup> destroyed the conjugation between the aromatic rings and a colorless compound was formed at low pH. In case of acid as well as alkaline regimes, these two nucleophiles exhibited the similar phenomenon of disrupting the conjugated diene system to terminate the quinone moiety of BG dye [23]. However, only pH variation did not have any effect on COD reduction.

### Determination of optimal pH and Fe<sup>2+</sup>/H<sub>2</sub>O<sub>2</sub> molar ratio

pH has a pivotal role in the decomposition of a contaminant in Fenton and Fenton-like reactions. Furthermore, the separation of Fe(III) species is strongly affected by the pH change. The role of pH in the Fenton reaction is commonly studied [23]. pH of a solution is likely to be in acidic range to generate the maximum amount of hydroxyl radicals. The

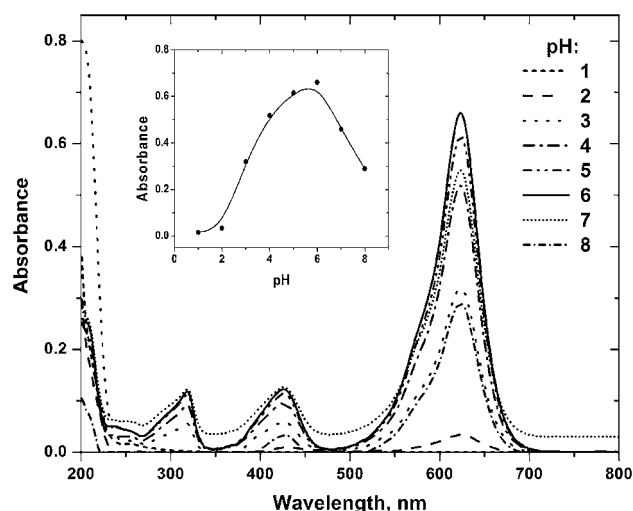


**Fig. 1** pH vs. absorption spectra with BG dye of 4 mg L<sup>-1</sup>. Inset figure variation of absorbance with pH at  $\lambda_{\max}$  623 nm

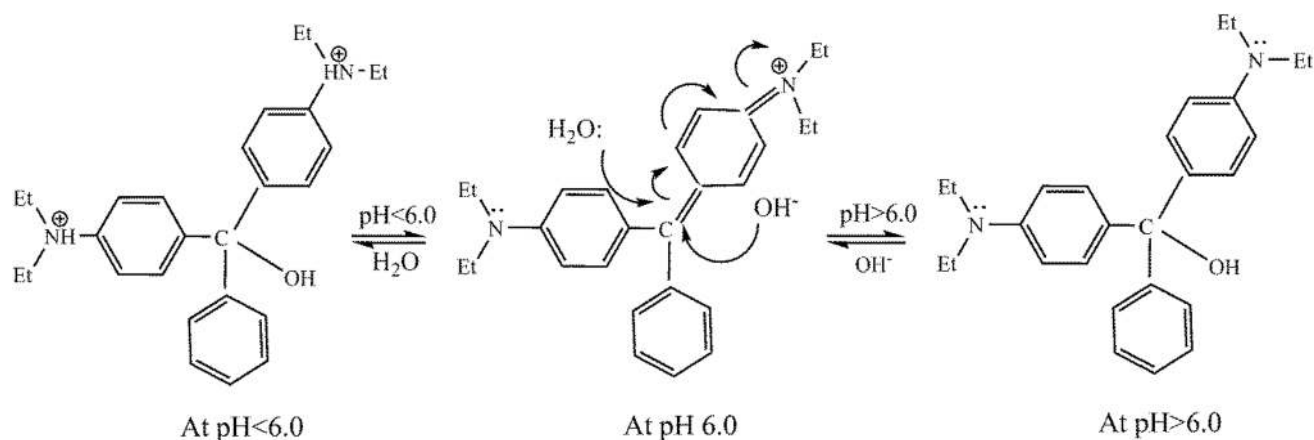


**Fig. 2** Structure of BG dye and effect of pH on its resonance stability

effect of pH on decolorization of BG dye at 270 rpm is shown in Fig. 3a. The stirring speed was set at 270 rpm after testing different agitation speeds from 150 to 350 rpm. The results showed about 7 % increase of dye removal by changing the stirrer speed from 150 to 270 rpm at pH 3.0 with  $50 \text{ mg L}^{-1}$  BG,  $56 \text{ mg L}^{-1}$   $\text{Fe}^{2+}$  and  $170 \text{ mg L}^{-1}$   $\text{H}_2\text{O}_2$  after 30 min of reaction. However, a further increase up to 350 rpm showed no significant improvement on the removal. Hence, the subsequent study was performed at 270 rpm. pH was varied from two with an increment of one unit up to six. Figure 3b presents the comparative color and COD reduction at 30 min of reaction. The highest amount dye was degraded at pH 3. Further pH elevation lowered BG decolorization. Generation of hydroxyl radicals is retarded due to the formation of ferric-hydroxo complexes typically at  $\text{pH} > 4$ .  $\text{H}_2\text{O}_2$  is also unstable in an alkaline solution. Thus, the application of Fenton reagent is restricted at  $\text{pH} > 7$  [11].

Considerably lower COD removal was noted than the corresponding decolorization. It may be corroborated by the yielding of organic fragments which was not being completely mineralized under oxidation conditions. Decolorization and COD removal dramatically increased from 54 to 95 and 47 to 77 % with the pH rise from 2 to 3 at 30 min, respectively. Further increase of pH up to 6, color, and COD removal dropped to 76 and 41 %, respectively. Henceforth, pH 3 was selected as the optimum value for subsequent studies.

The selection of an optimum  $\text{H}_2\text{O}_2$  concentration to achieve the maximum removal efficiency of a pollutant is an important factor associated with the treatment cost. Several studies have reported the existence of an optimum  $\text{H}_2\text{O}_2$  dosage. Nonetheless, there is no unified agreement on the ratio of  $\text{Fe(II)}$  to  $\text{H}_2\text{O}_2$  that gives the best results. Woo et al. [24] achieved 99 and 91 % reduction in color and COD at the optimum pH of 3.5,  $\text{Fe}^{2+}$  of 10 mM,  $\text{H}_2\text{O}_2$  of 40 mM ( $\text{Fe}^{2+}/\text{H}_2\text{O}_2$  mol ratio 1:4) with an initial Terasil

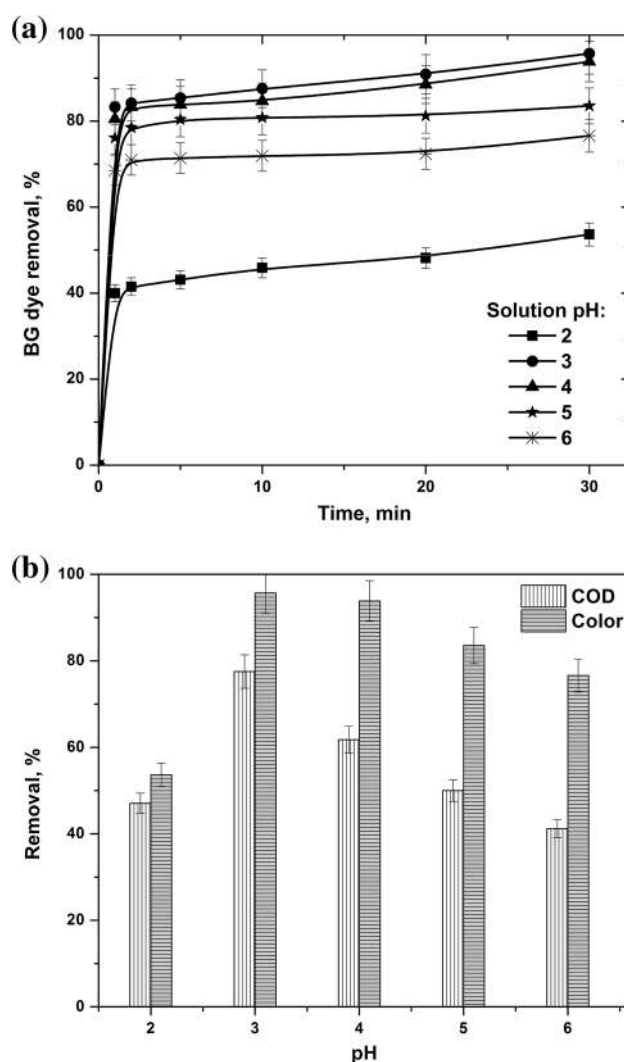


**Fig. 3** a BG dye decolorization kinetics at different pH, b effect of pH on dye decolorization and COD at 30 min of reaction. Experimental conditions: initial BG dye concentration  $100 \text{ mg L}^{-1}$ ,  $\text{Fe}^{2+}$  concentration  $56 \text{ mg L}^{-1}$ ,  $\text{H}_2\text{O}_2$  concentration  $170 \text{ mg L}^{-1}$ , agitation speed 270 rpm, temperature  $25 \pm 2 \text{ }^\circ\text{C}$  and solution volume 400 mL

Red R dye concentration of 0.23 mM. Lucas and Peres [25] obtained the similar optimal condition as pH 3,  $\text{Fe}^{2+}$  0.15 mM,  $\text{H}_2\text{O}_2$  0.73 mM ( $\text{Fe}^{2+}/\text{H}_2\text{O}_2$  mol ratio 1:4.9) and initial concentration 0.1 mM for the decomposition of Reactive Black 5. They reported around 97.5 and 21.6 % color and TOC removal.

The experiments were conducted by varying  $\text{Fe(II)}/\text{H}_2\text{O}_2$  molar ratio at a fixed pH and initial dye concentration to observe the optimal ratio.  $\text{Fe}^{2+}/\text{H}_2\text{O}_2$  molar ratio was varied as: 1:20 (0.25:5), 1:10 (0.5:5), 1:5 (1:5) and 1:10 (1:10). The molar ratio is given in the parenthesis, and the results are shown in Fig. 4. The majority of BG molecule was cleaved within 2.5 min. It is attributable to the predominant  $\bullet\text{OH}$  formation in the first stage of the reaction.  $\bullet\text{OH}$  is progressively transformed to  $\text{OH}^-$  leaving off  $\text{Fe}^{3+}$  and eventually the reaction is terminated. It is evident from Fig. S1 of the Supplementary Material that dye decomposition was enhanced notably with the increase of both  $\text{Fe}^{2+}$  and  $\text{H}_2\text{O}_2$  concentration at the same ratio. Nearly complete decolorization was achieved at a  $\text{Fe}^{2+}$  to  $\text{H}_2\text{O}_2$  molar ratio of 1:10 within of reaction 5 min. However, there was a little improvement on COD removal with doubling the concentration of  $\text{H}_2\text{O}_2$  (Fig. 4). It increased to 93 % at 1:10 from 91 % at 1:5. Therefore,  $\text{Fe}^{2+}/\text{H}_2\text{O}_2$  mol ratio of 1:5 was chosen for the rest of the investigations.

#### Comparative dye, COD and TOC removal at optimal condition

BG dye decolorization showed two distinct rate periods (Fig. 5), i.e., initial faster color removal followed by almost

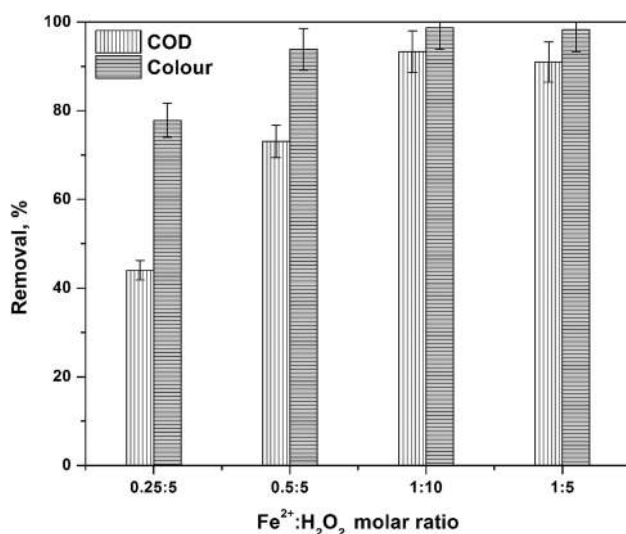


**Fig. 4** Color and COD removal for various molar ratios of  $\text{Fe}^{2+}/\text{H}_2\text{O}_2$  at 30 min. Experimental conditions: initial BG dye concentration  $50 \text{ mg L}^{-1}$ ,  $\text{Fe}^{2+}$  concentration  $56 \text{ mg L}^{-1}$ ,  $\text{H}_2\text{O}_2$  concentration  $170 \text{ mg L}^{-1}$ , pH 3, agitation speed 270 rpm, temperature  $25 \pm 2^\circ \text{C}$  and solution volume 400 mL

a constant rate period even though there was a sufficient amount of unreacted dye. Decolorization rate was faster at  $< 2$  min, and it attained the steady condition within 5 min. Whereas COD and TOC removal was increased even more gradually with the reaction time. The high initial rate of  $\bullet\text{OH}$  formation resulted faster dye (till 5 min), COD and TOC (till 20 min) removals. Maximum COD and TOC removal were found as 85 and 71 % in 20 min against the color removal of 87 %. After that, there was no notable effect of treatment time on color, COD, and TOC removal. Khuntia et al. [19] also obtained about 99 % decolorization and 80 % mineralization of BG dye in 40 and 60 min at neutral pH using ozone microbubbles.

The industrial dyeing effluents are laden with different background species like  $\text{Cl}^-$ ,  $\text{SO}_4^{2-}$ ,  $\text{PO}_4^{3-}$ ,  $\text{Na}^+$ ,  $\text{Ca}^{2+}$ ,  $\text{Mg}^{2+}$ , etc., [26–28]. Most of the times it reduces the treatment efficiency and also could influence the degradation pathways. The composition of industrial dyeing effluents from different sources is listed in Table S1 of the Supplementary Material. Likewise, the BG dye solution was spiked with common salts to achieve almost the similar composition of a real industrial dyeing effluent (Table S2 of the Supplementary Material). The results with and without background species are shown in Fig. 5. It is clear that the removal efficiency of BG dye, COD and TOC was inhibited in the presence background species commonly found in industrial dyeing effluent. There were about 89, 76 and 63 % of color, COD and TOC removal after 30 min of reaction in the presence of salts. It gave almost 9 % reductions in each color, COD, and TOC removal when compared to BG decomposition without background salts. Inhibition could occur due to complexation of  $\text{Fe(II)}/\text{Fe(III)}$  species with  $\text{Cl}^-$  and  $\text{SO}_4^{2-}$  ions.

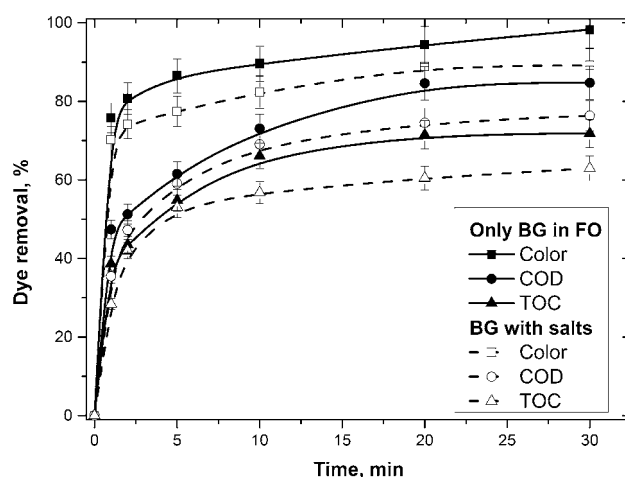
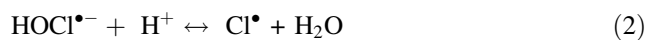


**Fig. 5** Effect of reaction time on color, COD and TOC removal at optimal condition with and without common ions. Experimental conditions: initial BG dye concentration  $50 \text{ mg L}^{-1}$ ,  $\text{Fe}^{2+}$  concentration  $56 \text{ mg L}^{-1}$ ,  $\text{H}_2\text{O}_2$  concentration  $170 \text{ mg L}^{-1}$ , pH 3, agitation speed 270 rpm, temperature  $25 \pm 2^\circ \text{C}$  and solution volume 400 mL

$\text{Cl}^-$  acts as  $\bullet\text{OH}$  radical scavenger (Eqs. (1) and (2)) resulting in the reduction of its availability. Apart from this,  $\text{Cl}^-$  ion has a strong affinity to coordinate with ferric ion forming a less reactive hexachloro-ferrate ( $\text{FeCl}_6^{3-}$ ) complex [29] which in turns could suppress  $\bullet\text{OH}$  formation.  $\text{SO}_4^{2-}$  also reacts with Fe(II) and Fe(III) ions producing  $\text{FeSO}_4$  and  $\text{Fe}_2(\text{SO}_4)_3$  that decreases the catalytic activity [30].



The difference in the rate of dye decolorization and TOC reduction is illustrated in Fig. S2 of the Supplementary Material. The decolorization rate was faster than mineralization at the beginning of the reaction, and it dropped almost linearly till 5 min of reaction. Subsequently, TOC removal rate was faster than the corresponding decolorization rate. The change in dye color is due to the loss of its conjugation which resulted in the formation of hydroquinone. It implies that the formation of hydroquinone and quinone derivatives was easier than splitting of dye into inorganic compounds.

### Enhancement of biodegradability index

The ratio of biochemical oxygen demand to chemical oxygen demands (BOD/COD), termed as biodegradability index, is an important indicator to study the nature of biodegradability [31]. The initial BOD<sub>5</sub> and COD were 13.3 and 78 mg L<sup>-1</sup> for an aqueous solution of 50 mg L<sup>-1</sup> BG dye. It implies the non-biodegradable nature of BG dye (BOD<sub>5</sub>/COD = 0.17). It is considered that wastewater containing coloring agents are reasonably biodegradable with BOD<sub>5</sub>/COD ≥ 0.4 [32, 33]. The biodegradability index (BOD<sub>5</sub>/COD) increased up to 0.49, i.e., with BOD<sub>5</sub> 3.43 and COD 7 mg L<sup>-1</sup>, when BG dye decolorization was about 98 % at the end of the run (Fig. 5). It implies that Fenton oxidation can be used as a pre-treatment step prior to biological treatment of textile effluent containing such azo dyes. He et al. [34] found that BOD<sub>5</sub>/COD of wastewater containing nitrobenzene increases from 0.03 to 0.47 in Fenton oxidation at pH 3, optimum H<sub>2</sub>O<sub>2</sub> to Fe<sup>2+</sup> mole ratio 9.9 and reaction time 150 min. Ramteke and Gogate [35] worked on the decomposition of *p*-nitrophenol and ethylbenzene using Fenton reagent. The BOD<sub>5</sub>/COD ratio increased to 0.297 and 0.355 from the initial values of 0.224 and 0.156.

### Mechanism of BG dye decomposition and formation of intermediates

LC–MS technique was used to determine intermediates formed during cleavage of BG molecule as well as to

understanding the mechanism of dye degradation. The mass-to-charge ratio (*m/z*) of important intermediates detected in mass spectra is shown in Fig. 6. It shows that BG molecule was cleaved into 12 fragments. The possible pathways of their formation are illustrated in Fig. 7a. The error in *m/z* is computed from its difference between the proposed and exact values (Table 1).

Fairly low errors (−0.88 to 0.49 g mol<sup>-1</sup>) in the proposed mass of the fragments were obtained (Fig. 7a; Table 1). Hydroquinone, i.e., 1,4-dihydroxy benzene was formed which is very susceptible to get oxidized [36], and *p*-benzoquinone was originated from this compound. The central carbon atom has nucleophilic character due to the presence of two bulky electron-donating groups. ‘D’ following a subscript denotes degradation products. D<sub>1</sub> (*N,N*-diethyl aniline) was yielded by an electrophilic attack [37] at the more nucleophilic carbon atom. D<sub>2</sub> molecule appeared by the substitution of  $\bullet\text{OH}$  radical at *p*-position with respect to the diethylamine group (−Et<sub>2</sub>N) of D<sub>1</sub> as this group is ortho (−o) and para (−p) orienting. The o-product has a lower possibility of the formation because of steric hindrance [38] between diethyl amine and −OH groups. Successive hydroxylation of D<sub>2</sub> molecule at o-position followed by a reaction between two −OH groups and NaOH yielded D<sub>3</sub> with quite low error (−0.05 g mol<sup>-1</sup>). Hence, two −OH groups are converted to Na-salts of phenoxide ion because of the addition of NaOH during  $\bullet\text{OH}$  radical quenching at different time intervals. D<sub>4</sub>, an aromatic ketone compound, was originated by an electrophilic attack of  $\bullet\text{OH}$  radicals with the disappearance of the quinone structure. The color of BG is due to the presence of quinone structure [8]. D<sub>4</sub> was further oxidized to benzoic

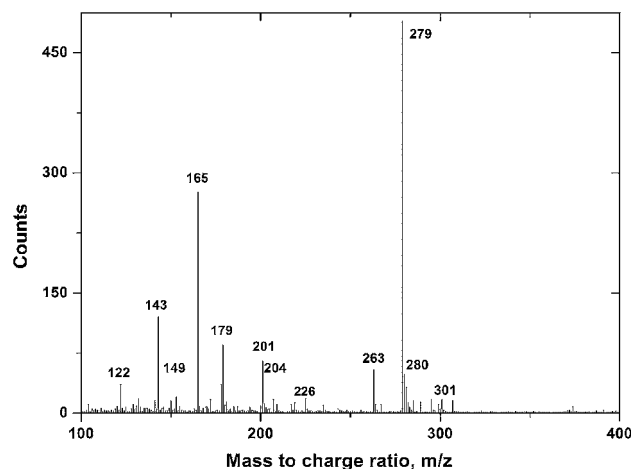


**Fig. 6** MS spectra acquired in Fenton oxidation of BG dye at 30 min of reaction time. Experimental conditions: initial BG concentration 50 mg L<sup>-1</sup>, Fe<sup>2+</sup> concentration 56 mg L<sup>-1</sup>, H<sub>2</sub>O<sub>2</sub> concentration 340 mg L<sup>-1</sup>, Fe<sup>3+</sup> concentration 56 mg L<sup>-1</sup>, pH 3, agitation speed 270 rpm, temperature 25 ± 2 °C and solution volume 400 mL

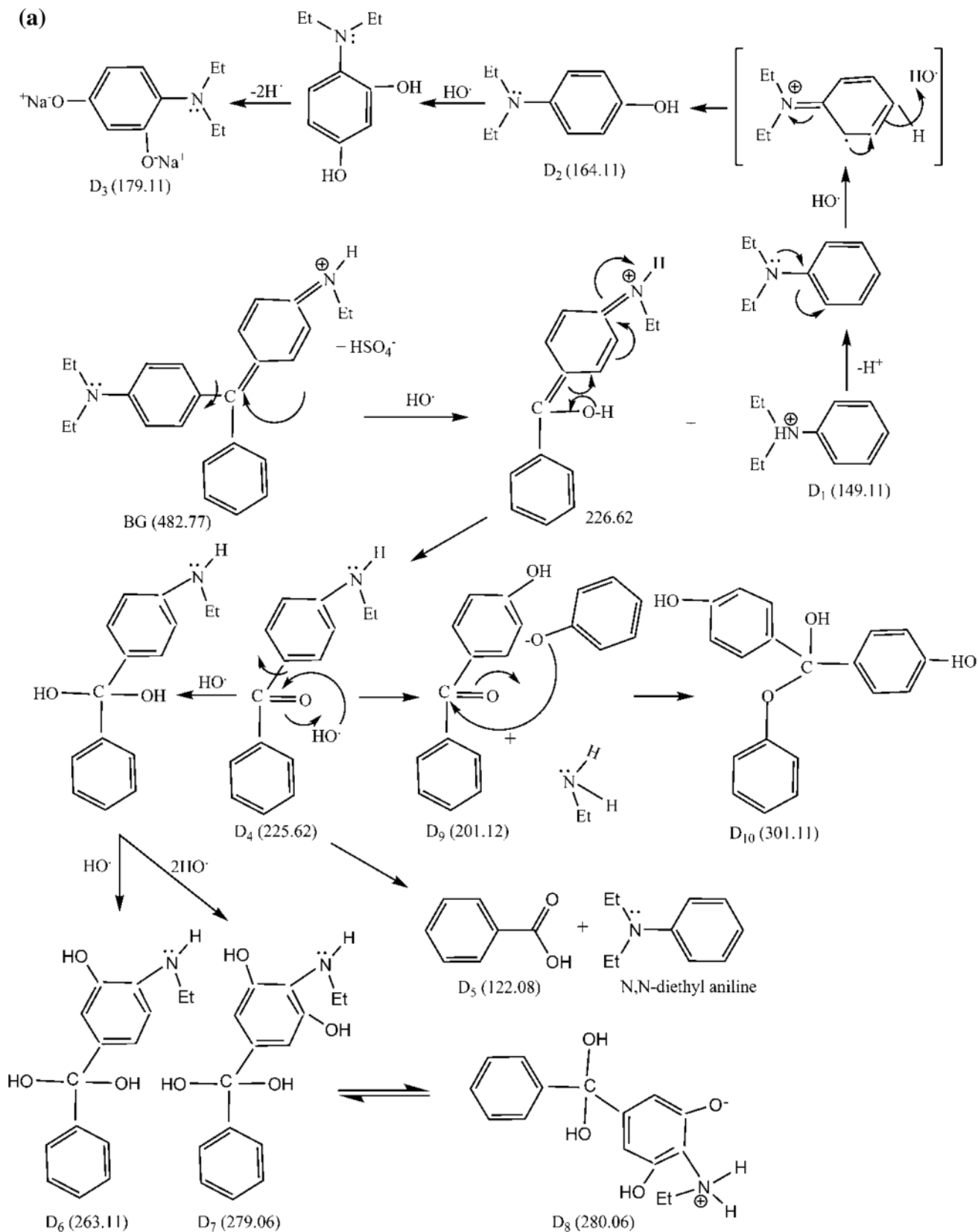


**Fig. 7 a** Pathways of BG dye degradation and formation intermediates. Experimental conditions: initial BG concentration 50 mg L<sup>-1</sup>, Fe<sup>2+</sup> concentration 56 mg L<sup>-1</sup>, H<sub>2</sub>O<sub>2</sub> concentration 340 mg L<sup>-1</sup>, pH

3, agitation speed 270 rpm, temperature 25 ± 2 °C and solution volume 400 mL. **b** Pathways for formation of intermediates found with common ions. **c** Formation of Fe(III)-hydroquinone chelate

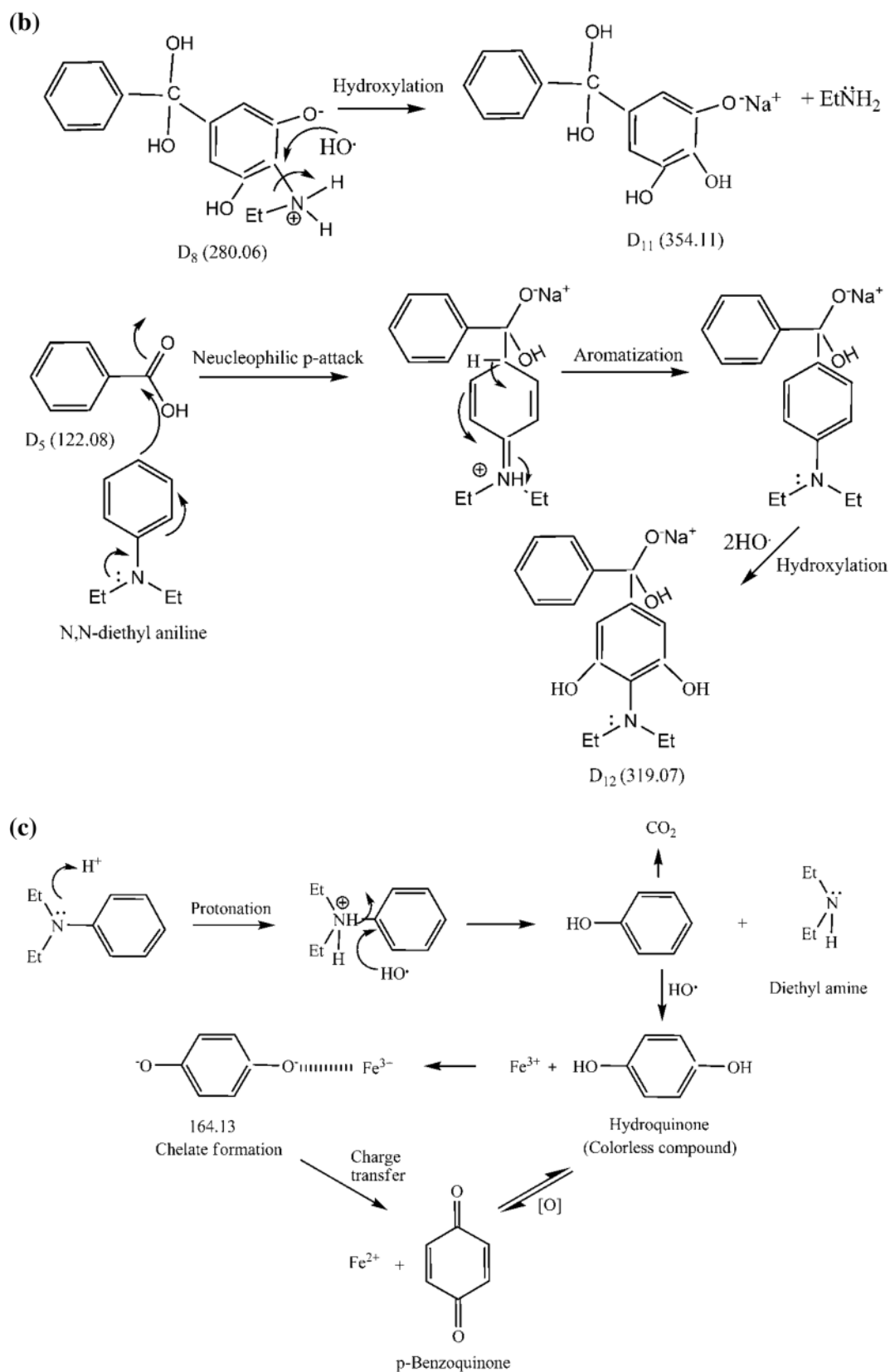


Fig. 7 continued



**Table 1** Mass-to-charge ratio ( $m/z$ ) of the intermediates from proposed decomposition mechanism and its error with respect to exact  $m/z$ 

Fragment	Structure	Mass-to-charge ratio	Error ( $\text{g mol}^{-1}$ )
D <sub>1</sub>	C <sub>10</sub> H <sub>17</sub> N	149.09	0.02
D <sub>2</sub>	C <sub>10</sub> H <sub>17</sub> NO	164.99	−0.86
D <sub>3</sub>	C <sub>8</sub> H <sub>14</sub> NO <sub>2</sub>	179.16	−0.05
D <sub>4</sub>	C <sub>15</sub> H <sub>20</sub> O <sub>2</sub>	225.13	0.49
D <sub>5</sub>	C <sub>8</sub> H <sub>12</sub> N	122.11	−0.03
D <sub>6</sub>	C <sub>16</sub> H <sub>16</sub> O <sub>3</sub> N	263.13	−0.02
D <sub>7</sub>	C <sub>16</sub> H <sub>16</sub> NO <sub>4</sub>	279.18	−0.12
D <sub>8</sub>	C <sub>15</sub> H <sub>22</sub> NO <sub>4</sub>	280.2	−0.14
D <sub>9</sub>	C <sub>13</sub> H <sub>13</sub> O <sub>2</sub>	201.12	0
D <sub>10</sub>	C <sub>19</sub> H <sub>20</sub> O <sub>3</sub>	301.17	−0.06

acid (D<sub>5</sub>) along with *N,N*-diethyl aniline. D<sub>6</sub> and D<sub>7</sub> were originated from D<sub>4</sub> molecule by hydroxylation at central carbon because of more electrophilic nature for any nucleophilic reaction. D<sub>8</sub> was formed simply by protonation of D<sub>7</sub>. D<sub>9</sub> appeared by the direct substitution of  $\bullet\text{OH}$  radical with the release of  $-\text{Et}_2\text{N}$  group. The proposed mass of this compound exactly matched the actual mass in mass spectra. D<sub>10</sub> was originated by a nucleophilic attack of the phenoxide group at the more electrophilic center of D<sub>9</sub> with the loss of ethyl amine molecule.

The mass spectra obtained with background species is shown in Fig. S3 of the Supplementary Material. A comparison between Figs. 6 and S3 (Supporting Information) reveals that most of the degradation products were common in both the processes. However, two additional intermediates were identified with  $m/z$  of 254.16 (D<sub>11</sub>) and 319 (D<sub>12</sub>) in the presence of background species. D<sub>11</sub> was formed on hydroxylation of D<sub>8</sub> compound after removal of bulky ethylamine group (Fig. 7b). The substitution reaction occurred easily by  $\bullet\text{OH}$  radical because of steric hindrance [39] between bulky amine and  $-\text{OH}$  groups. D<sub>12</sub> was originated as an additive product by the nucleophilic attack of *N,N*-diethyl aniline (from the para position) and the D<sub>5</sub> molecule (Fig. 7b). The carbonyl center of  $-\text{COOH}$  group in D<sub>5</sub> acted as an electrophile [40].

It is seen that Fenton oxidation could effectively reduce the color of BG dye. COD reduction was about 7 % less in comparison to decolorization as in Fig. 5. It is due to possible of the formation of different iron chelate including hydroquinone, and quinone compounds. Hydroxylation of *N,N*-diethyl aniline yielded hydroquinone and the path of its formation is shown in Fig. 7c. Hydroquinone has equal probability to react with  $\text{Fe}^{3+}$  as well as to get oxidized to quinone through a redox cycle between quinone and hydroquinone and,  $\text{Fe}^{3+}$  and  $\text{Fe}^{2+}$ . Fe(III)-hydroquinone chelate complex is likely to be more stable because of less stability of quinone. Such iron-complexes usually exhibit

resistance to further degradation in Fenton and Fenton-like reactions. This explains the lower COD removal than the decolorization [41, 42].

## Conclusions

The study on Brilliant Green (BG) dye signifies that Fenton oxidation is a promising treatment option for decolorization and mineralization of coloring components from wastewater. The following conclusions are drawn from the present work:

- The green appearance of BG dye is due to the presence of quinone moiety. pH greatly influenced the absorption intensity of BG solution due to disruption of an extended conjugated system and the maximum absorbance was observed at pH 6.
- The optimal pH and molar ratio of  $\text{Fe}^{2+}/\text{H}_2\text{O}_2$  were found as 3 and 1:5. The maximum color and COD removals were 98 and 91 % of 50 mg L<sup>−1</sup> BG dye at 30 min of oxidation time. The unreacted dye exhibited negative synergy on COD removal.
- The addition of common ions in dye solution similar to that in an industrial effluent caused more or less 9 % reduction in dye color and mineralization efficiencies.
- Biodegradability index (BOD<sub>5</sub>/COD) augmented to 0.49 after 30 min of oxidation from its initial value of 0.17 with 50 mg L<sup>−1</sup> BG dye.
- The central carbon atom of BG molecule acts as a nucleophilic center in the presence of two bulky electron-donating groups. Dye decomposition was initiated with an electrophilic attack at the more nucleophilic center.
- A redox cycle was established between quinone/hydroquinone and  $\text{Fe}^{3+}/\text{Fe}^{2+}$  system. Lower COD removal than decolorization could be explained by more stability of Fe(III)-hydroquinone chelate which was resistant to further decomposition in Fenton oxidation.

**Open Access** This article is distributed under the terms of the Creative Commons Attribution 4.0 International License (<http://creativecommons.org/licenses/by/4.0/>), which permits unrestricted use, distribution, and reproduction in any medium, provided you give appropriate credit to the original author(s) and the source, provide a link to the Creative Commons license, and indicate if changes were made.

## References

1. Turabik M, Gozmen B (2013) Removal of basic textile dyes in single and multi-dye solutions by adsorption: statistical



- optimization and equilibrium isotherm studies. *CLEAN Soil Air Water* 6:1080–1092
2. Nandi BK, Goswami A, Purkait MK (2009) Removal cationic dyes from aqueous solutions by kaolin: kinetic and equilibrium studies. *Appl Clay Sci* 42:583–587
  3. Sivraj R, Namasivayam C, Kadirvelu K (2001) Orange peel as an adsorbent in the removal of acid violet 17 (acid dye) from aqueous solution. *Waste Manag* 21:105–109
  4. Pang YL, Abdullah AZ (2013) Current status of textile industry wastewater management and research progress in Malaysia: a review. *CLEAN Soil Air Water* 41:751–764
  5. Arslan I, Balcioglu IA (1999) Degradation of commercial reactive dyestuffs by heterogeneous and homogenous advanced oxidation processes: a comparative study. *Dyes Pigment* 43:95–108
  6. Galindo C, Jacques P, Kalt A (2001) Photooxidation of the phenylazonaphthol AO20 on TiO<sub>2</sub>: kinetic and mechanistic investigations. *Chemosphere* 45:997–1005
  7. Slokar YM, Marechal AML (1998) Methods of decoloration of textile wastewaters. *Dyes Pigment* 37:335–356
  8. Konstantinou IK, Albanis TA (2004) TiO<sub>2</sub>-assisted photocatalytic degradation of azo dyes in aqueous solution: kinetic and mechanistic investigations: a review. *Appl Catal B Environ* 49:1–14
  9. Munter R (2001) Advanced oxidation processes—current status and prospects. *Proc Estonian Acad Sci Chem* 50:59–80
  10. Sun C, Chen C, Ma W, Zhao J (2011) Photodegradation of organic pollutants catalysed by iron species under visible light irradiation. *Phys Chem Chem Phys* 13:1957–1969
  11. Kuo WG (1992) Decolorizing dye wastewater with Fenton's reagent. *Water Res* 26:881–886
  12. Kang N, Lee DS, Yoon J (2002) Kinetic modeling of Fenton oxidation of phenol and mono chlorophenols. *Chemosphere* 47:915–923
  13. Liu H, Chen Q, Yu Y, Liu Z, Xue G (2013) Influence of Fenton's reagent doses on the degradation and mineralization of H-acid. *J Hazard Mater* 263:593–599
  14. Roy G, Donato P, Gorner T, Barres O (2003) Study of tropaeolin degradation by iron-proposition of a reaction mechanism. *Water Res* 37:4954–4964
  15. Styliidi M, Kondarides DI, Verykios XE (2003) Pathways of solar light-induced photocatalytic degradation of azo dyes in aqueous TiO<sub>2</sub> suspensions. *Appl Catal B* 43:271–286
  16. Gogate PR, Bhosale GS (2013) Comparison of effectiveness of acoustic and hydrodynamic cavitation in combined treatment schemes for degradation of dye wastewaters. *Chem Eng Process* 71:59–69
  17. Shirsath SR, Patil AP, Patil R, Naik JB, Gogate PR, Sonawane SH (2013) Removal of Brilliant Green from wastewater using conventional and ultrasonically prepared poly(acrylic acid) hydrogel loaded with kaolin clay: a comparative study. *Ultrason Sonochem* 20:914–923
  18. Gole VL, Gogate PR (2014) Degradation of Brilliant Green dye using combined treatment strategies based on different irradiations. *Sep Purif Technol* 133:212–220
  19. Khuntia S, Majumdera SK, Ghosh P (2015) A pilot plant study of the degradation of Brilliant Green dye using ozone microbubbles: mechanism and kinetics of reaction. *Environ Technol* 36:336–347
  20. Hashemian S (2013) Fenton-like oxidation of Malachite green solutions: kinetic and thermodynamic study. *J Chem* 2013:1–7
  21. Munoz RA, Kolbe M, Siloto RC, Oliveira PV, Angnes L (2007) Ultrasound-assisted treatment of coconut water samples for potentiometric stripping determination of Zinc. *J Braz Chem Soc* 18:410–415
  22. Das RK, Golder AK (2013) Stability of aqueous H<sub>2</sub>O<sub>2</sub> at elevated temperature and pH in presence of common cations. In: Indian chemical engineering congress-2013 (CHEMCON-13), p 388
  23. Ertugay N, Acar FN (2013) Removal of COD and color from Direct Blue 71 azo dye wastewater by Fenton's oxidation: kinetic study. *Arab J Chem*. doi:10.1016/j.arabjc.2013.02.009
  24. Woo YS, Rafatullah M, Al-Karkhi AFM, Tow TT (2014) Removal of Terasil Red R dye by using Fenton oxidation: a statistical analysis. *Desalin Water Treat* 52:4583–4591
  25. Lucas MS, Peres JA (2006) Decolorization of the azo dye Reactive Black 5 by Fenton and photo-Fenton oxidation. *Dyes Pigment* 71:236–244
  26. Rajesh VK (2013) Microbiological research in agroecosystem management. Springer, New York
  27. Fulekar MH (2010) Bioremediation technology: recent advances. Springer, New York
  28. Jolly YN, Islam A (2009) Characterization of dye industry effluent and assessment of its suitability for irrigation purpose. *J Bangladesh Acad Sci* 33:99–106
  29. Giri AS, Golder AK (2015) Drug mixture decomposition in photo-assisted Fenton process: comparison to singly treatment, evolution of inorganic ions and toxicity assay. *Chemosphere* 127:254–261
  30. Sarkar RP (2012) General and inorganic chemistry part 1. New Central Book Agency (P) Ltd, India
  31. Neill CO, Hawkes FR, Hawkes DL, Lourenco ND, Pinheiro HM, Delee W (1999) Colour in textile effluents-sources, measurement, discharge consents and simulation: a review. *J Chem Technol Biotechnol* 74:1009–1018
  32. Chun H, Yizhong W (1999) Decolorization and biodegradability of photocatalytic treated azo dyes and wool wastewater. *Chemosphere* 39:2107–2115
  33. Gilbert E (1987) Biodegradability of ozonation products as a function of COD and DOC elimination by example of substituted aromatic substances. *Water Res* 21:1273–1278
  34. He S, Wang L, Jie Z, Hou M (2009) Fenton pre-treatment of wastewater containing nitrobenzene using ORP for indicating the endpoint of reaction. *Procedia Earth Planet Sci* 1:1268–1274
  35. Ramteke LP, Gogate PR (2015) Removal of ethylbenzene and p-nitrophenol using combined approach of advanced oxidation with biological oxidation based on the use of novel modified prepared activated sludge. *Process Saf Environ* 95:146–158
  36. Gao J, Jie Y, Yan L, Xiaoyan H, Lili B, Lumei P, Wu Y, Quanfang L, Zhiming Y (2006) Decoloration of aqueous brilliant green by using glow discharge electrolysis. *J Hazard Mater* 137:431–451
  37. Chen JS, Liu MC, Zhang JD, Xian YZ, Jin LT (2003) Electrochemical degradation of bromopyrogallol red in presence of cobalt ions. *Chemosphere* 53:1131–1136
  38. Sykes Peter (2003) A guidebook to mechanism in organic chemistry, 6th edn. Pearson, Cambridge
  39. Finar IL (2001) Stereochemistry and the chemistry of natural products, 5th edn. Holloway, London
  40. Hesse M, Meier H, Zeeh B (2008) Spectroscopic methods in organic chemistry, 2nd edn. Thieme, New York
  41. Pradeep K, Prasad B, Mishra IM, Chand S (2008) Decolorization and COD reduction of dyeing wastewater from a cotton textile mill using thermolysis and coagulation. *J Hazard Mater* 153:635–645
  42. Hyunhee L, Makoto LS (2008) Removal of COD and color from livestock wastewater by the Fenton method. *J Hazard Mater* 153:1314–1319